Published in final edited form as:

Oncogene. 2015 May 21; 34(21): 2721–2731. doi:10.1038/onc.2014.226.

Autocrine CSF1R signaling mediates switching between invasion and proliferation downstream of TGFβ in claudin-low breast tumor cells

Antonia Patsialou[1,4], **Yarong Wang**[1,2], **Jeanine Pignatelli**[1], **Xiaoming Chen**[1], **David Entenberg**[1,2], **Maja Oktay**[3], and **John S. Condeelis**[1,2]

[1]Department of Anatomy and Structural Biology, Albert Einstein College of Medicine

[2]Gruss Lipper Biophotonics Center, Albert Einstein College of Medicine, Bronx, NY 10461, USA

[3]Department of Pathology, Montefiore Medical Center, Bronx, NY, 10467, USA

Abstract

Patient data suggest that colony stimulating factor-1 (CSF1) and its receptor (CSF1R) play critical roles during breast cancer progression. We have previously shown that in human breast tumors expressing both CSF1 and CSF1R, invasion in vivo is dependent both on a paracrine interaction with tumor-associated macrophages and an autocrine regulation of CSF1R in the tumor cells themselves. Although the role of the paracrine interaction between tumor cells and macrophages has been extensively studied, very little is known about the mechanism by which the autocrine CSF1R signaling contributes to tumor progression. We show here that breast cancer patients of the claudin-low subtype have significantly increased expression of CSF1R. Using a panel of breast cancer cells lines, we confirm that CSF1R expression is elevated and regulated by TGFβ specifically in claudin-low cell lines. Abrogation of autocrine CSF1R signaling in MDA-MB-231 xenografts (a claudin-low cell line) leads to increased tumor size by enhanced proliferation, but significantly reduced invasion, dissemination and metastasis. Indeed, we show that proliferation and invasion are oppositely regulated by CSF1R downstream of TGFβ only in claudin-low cells lines. Intravital multiphoton imaging revealed that inhibition of CSF1R in the tumor cells leads to decreased in vivo motility and a more cohesive morphology. We show that, both in vitro and in vivo, CSF1R inhibition results in a reversal of claudin-low marker expression by significant upregulation of luminal keratins and tight junction proteins such as claudins. Finally, we show that artificial overexpression of claudins in MDA-MB-231 cells is sufficient to tip the cells from an invasive state to a proliferative state. Our results suggest that autocrine CSF1R signaling is

Correspondence should be addressed to Antonia Patsialou: 72 Huntley Street, UCL Cancer Institute, University College London, London WC1E 6DD, UK. Tel: + 442076790735, Fax: + 442076796925, a.patsialou@ucl.ac.uk. And John Condeelis: 1301 Morris Park Avenue, Albert Einstein College of Medicine, Bronx, NY 10461, USA. Tel: + 17186781126, Fax: + 17186781128, john.condeelis@einstein.yu.edu.

[4]Present address: University College London, Research Department of Cancer Biology, London WC1E 6DD, UK.

CONFLICT OF INTEREST

Condeelis holds equity and is a consultant for MetaStat and is a consultant for Deciphera Pharmaceuticals. Entenberg is a consultant for MetaStat. The other authors declare no conflict of interest.

Supplementary Information accompanies the paper on the Oncogene website (http://www.nature.com/onc)

essential in maintaining low claudin expression and that it mediates a switch between the proliferative and the invasive state in claudin-low tumor cells downstream of TGFβ.

Keywords

CSF1R; claudin-low breast cancer; invasion; metastasis

INTRODUCTION

Breast cancer is one of the most frequent malignant neoplasms occurring in women in developed countries. Recent advances in genomic analysis have greatly advanced our understanding of the heterogeneity of this disease. Five main “intrinsic” subtypes have been distinguished based on unsupervised clustering of gene expression profiles: the luminal-A cancers which are mostly estrogen receptor (ER)-positive and histologically low-grade; the luminal-B cancers which are also mostly ER-positive but often high-grade; the HER2-positive cancers which show high expression of the ERBB2 gene; the basal-like breast cancers which are mostly ER-negative, progesterone-receptor (PR)–negative, and HER2-negative (hence, “triple-negative”); and the newly recognized claudin-low subtype [1–5]. The claudin-low subtype is constituted mostly of triple negative tumors that show low expression of luminal differentiation markers, such as tight and adherens junction proteins, cadherins and claudins 3, 4 and 7 (hence the name “claudin-low”) [6, 7]. These molecular subtypes show different prognostic outcome as well as treatment sensitivities. However, their use in the clinic has been hindered by technical challenges such as the development of standardized cross-lab assays [8, 9]. Despite this, their unique molecular profiles are most likely due to the involvement of different signaling pathways, and information on such pathways would be useful for assessing prognostic applications and the specification of subtype-specific drugs.

Colony stimulating factor-1 (CSF1) and its receptor (CSF1R) have been associated with adverse prognostic outcome in tumors of the female reproductive system and other solid tumors [10–15]. In breast cancer, intravital multiphoton imaging of both transgenic and xenograft mouse models has shown that macrophages are obligate partners of invasion in the primary tumor [16–18]. CSF1 signaling to the macrophages is essential for this function: genetic ablation of CSF1 in the mammary cancer-susceptible MMTV-PyMT mice delays tumor progression and metastasis [19], while inhibition of CSF1R by blocking antibodies reduces in vivo tumor cell invasion of tumor cells [16, 17]. Blockade of CSF1 signaling to the macrophages has also been shown to reduce primary tumor growth due to decreased angiogenesis [20, 21], as well as to improve chemotherapeutic efficacy due to increased antitumor T-cell responses [22]. Interestingly, in humans, CSF1 and CSF1R are co-expressed in the tumor cells of patients [12, 23], raising the hypothesis that autocrine CSF1R signaling to tumor cells is also important in breast cancer progression. Several studies have now shown that tumor cell lines with artificial overexpression of both CSF1 and CSF1R exhibit increased motility and invasiveness in vitro [24–26]. We have previously shown that in MDA-MB-231, which spontaneously express both CSF1 and CSF1R without further manipulation, invasion in vivo occurs both through an EGF/CSF1 paracrine interaction with the

macrophages (similar to what was previously reported from mouse mammary tumor studies), and an autocrine CSF1/ CSF1R loop in the tumor cells [27].

The above studies argue that CSF1R signaling has great potential as a therapeutic target in breast cancer. Indeed, multiple companies are now investing in developing compounds that would inhibit CSF1R function and several of these compounds are already in clinical trials. However, although extensive data exist on the role of CSF1R in metastatic progression through its role in tumor-associated macrophages, very little is known about the role of autocrine CSF1R signaling in the tumor cells. This knowledge will be instrumental to our in depth understanding of CSF1R signaling in human breast tumor progression.

RESULTS

Claudin-low breast tumor cells express higher levels of CSF1R regulated by TGFβ

Breast tumors of different intrinsic subtypes are characterized by different gene expression profiles. We were interested in testing whether autocrine CSF1R signaling was correlated with a particular breast cancer subtype. We analyzed a publicly available breast cancer patient cohort (UNC337 database) [7], and found that CSF1R mRNA was expressed at significantly higher levels in claudin-low patients (Figure 1A). We also analyzed the mRNA expression levels for the ligand CSF1 and found again that claudin-low patients had slightly but significantly higher levels (Figure 1A). This suggests that autocrine CSF1R signaling may be more prominent in claudin-low breast cancer cells.

In order to investigate this further, and because patient data are extracted from whole tissue that contains stroma as well as tumor cells, we tested a panel of breast cancer cell lines representative of the various molecular subtypes (as classified in [7]). We found that the claudin-low cell lines (MDA-MB-231, Hs578T and BT549) had higher CSF1R expression than the luminal cell lines (MCF7 and T47D) (Figure 1B–C and Supplementary Figure 1). The basal-like cell line MDA-MB-468 also showed high expression of CSF1R (Figure 1B–C), an observation that was dissimilar to the patient data of Figure 1A. As far as CSF1 is concerned, we found again that the claudin-low cell lines expressed higher mRNA levels (Figure 1B–C), similar to the patient data of Figure 1A. We have previously shown that in MDA-MB-231 cells the CSF1/CSF1R autocrine loop is enhanced in vivo due to CSF1R upregulation mediated by TGFβ [27]. We sought to investigate if this was a property of all claudin-low breast cancer cells. We found that CSF1R mRNA was significantly upregulated after TGFβ stimulation in all three claudin-low cell lines tested, but not in the luminal or basal-like lines (although steady-state levels of CSF1R mRNA in MDA-MB-468 cells were similar to claudin-low cells) (Figure 1D). The mRNA levels of CSF1 were unchanged by TGFβ stimulation in all cell lines (Figure 1D), suggesting that the main regulation of the autocrine loop by TGFβ happens through transcription of the receptor and not the ligand. As a control, we confirmed that all cell lines, with the exception of T47D, were successfully stimulated by TGFβ (Supplementary Figure 2). In order to verify that CSF1R expression is directly downstream of TGFβ, we examined the CSF1R mRNA levels after knockdown of Smad3, a signaling molecule downstream of the TGFβ receptor. Smad3 knockdown in MDA-MB-231 cells abrogated CSF1R upregulation by TGFβ stimulation, while having no effect in MDA-MB-468 cells (Figure 1E), suggesting again that CSF1R is regulated by

TGFβ specifically in claudin-low breast cancer. Claudin-low breast cancer has been shown before to express a molecular profile enriched in TGFβ signaling [28], and we confirmed here that patients of the claudin-low subtype have significantly higher expression of TGFβ receptors 1 and 2 (TGFBR1 and TGFBR2) (Supplementary Figure 3), suggesting that the claudin-low tumor cells are presumably more responsive to exogenous TGFβ stimulation. These data taken together imply that autocrine CSF1R signaling is more prominent in claudin-low breast tumor cells and is regulated by TGFβ.

Autocrine CSF1R signaling attenuates proliferation of claudin-low breast cancer cells in vivo and in vitro

In order to investigate further the role of autocrine CSF1R signaling in claudin-low breast tumor cells, we generated stable CSF1R knockdown MDA-MB-231 cells expressing two different shRNA sequences, KD1 and KD2 (80% and 70% knockdown respectively, Supplementary Figure 4). When injected orthotopically in mice, CSF1R knockdown cells grew significantly larger tumors than control cells (Figure 2A). This effect was seen only in vivo, as KD1 and KD2 cells did not show a growth advantage in standard cell culture (Supplementary Figure 4). We found that the enlarged size of KD1 and KD2 tumors was due to increased cell proliferation, as measured by immunohistochemistry for ki67 (Figure 2B). We found no difference in apoptosis in these tumors (Supplementary Figure 5), suggesting that apoptosis did not contribute to the tumor size difference.

We sought to further investigate this observation by acute inhibition of the cancer cells' CSF1R after the tumor is established. Since macrophages also express CSF1R, and because we wanted to specifically address the role of autocrine CSF1R signaling in this study, we used a technique that we have successfully used in the past to differentiate between the autocrine and paracrine CSF1R signaling [27]. Since the human breast tumor is growing in a mouse host, an inhibitory antibody specifically recognizing the human CSF1R blocks only the autocrine signaling, while an inhibitory antibody specific to the mouse CSF1R blocks only the paracrine signaling with the macrophages (we validated the antibodies in [27]). When parental MDA-MB-231 tumors were treated with the anti-human CSF1R inhibitory antibody in vivo, proliferation was significantly increased, as evident by immunohistochemistry of tumor sections for two proliferation markers, ki67 and BrdU (Figure 2C). As a control, the anti-mouse CSF1R antibody did not affect proliferation in vivo (ki67 expression difference not significant, BrdU incorporation slightly decreased) (Figure 2C). No difference in apoptosis was observed between treatments (Supplementary Figure 5). Overall, both by shRNA silencing and antibody inhibition, our results indicate that autocrine CSF1R contributes to attenuation of tumor cell proliferation in vivo.

We next sought to determine whether the CSF1R–dependent proliferation attenuating phenotype was common to other claudin-low cells. When MDA-MB-231 cells were treated with the inhibitory anti-human CSF1R antibody in vitro, we found no difference in proliferation, as measured with an S-phase cell cycle progression assay by EdU incorporation (Figure 3A). We have previously found that autocrine CSF1R signaling in MDA-MB-231 cells is prominent only in vivo and is mediated by TGFβ [27]. Thus, to imitate the in vivo environment, we repeated the above experiment in the presence of TGFβ. In

breast cancer, TGFβ has been shown to act as a growth inhibitor specifically in ER-negative cancer cells [29, 30]. We show here that indeed in vitro proliferation of MDA-MB-231 cells (an ER-negative cell line) was significantly reduced in the presence of TGFβ (Figure 3A). Interestingly, inhibition of CSF1R in this setting released the growth inhibitory effect of TGFβ and resulted in increased proliferation (Figure 3A). We tested the panel of breast cancer cell lines in the same assay. Overall, the different cell lines had variable proliferation rates with no discernible pattern correlated to their subtype or CSF1R expression levels (Figure 3B). We found that proliferation of the claudin-low cell lines Hs578T and BT549 was arrested by TGFβ stimulation similar to MDA-MB-231, and that this arrest was released after inhibition of CSF1R (Figure 3C). However, the cells lines of the basal-like and luminal subtypes did not show the same phenotype, with no significant effect in EdU incorporation after TGFβ stimulation and a slight decrease in the presence of the anti-human CSF1R antibody (Figure 3C). Others have also reported that inhibition of CSF1R leads to decreased in vitro proliferation of MDA-MB-468 cells via ERK1/2 signaling, but claudin-low cell lines were not tested in that study [31]. We show here that autocrine CSF1R signaling is essential for the growth inhibition phenotype downstream of TGFβ in claudin-low breast tumor cells.

Autocrine CSF1R signaling enhances invasion and metastasis of claudin-low breast cancer in vivo and in vitro

We next sought to investigate the role of autocrine CSF1R signaling in metastatic progression of breast cancer cells. We analyzed orthotopic tumors generated from the CSF1R knockdown cells, KD1 and KD2, compared to equal size control tumors for their invasive and metastatic properties. We found that, compared to control, both KD1 and KD2 tumors showed significantly reduced invasion towards EGF (Figure 4A), reduced numbers of circulating tumor cells in the peripheral blood (Figure 4B), as well as reduced lung metastasis (Figure 4C). Since macrophages are essential for invasion and metastasis [32], we tested for the numbers of infiltrating macrophages in control, KD1 and KD2 tumors and found no significant difference (Supplementary Figure 6). Finally, when we measured experimental metastasis, where tumor cells are artificially introduced in the blood circulation bypassing invasion and intravasation, we found that lung metastasis now appeared increased for the KD1 cells (Figure 4D), in agreement with these cells having enhanced growth (Figure 2).

In order to study further the role of autocrine CSF1R signaling in in vivo invasion, we used intravital multiphoton imaging to visualize migration and invasion in primary tumors at single-cell resolution in real-time. We treated mice bearing orthotopic tumors of MDA-MB-231 cells with either a control IgG or the inhibitory anti-human CSF1R antibody, after which we imaged the tumors by multiphoton microscopy. Tumor cells were visualized by stable GFP expression, blood vessels by intravenous injection of fluorescent dextrans and collagen fibers by second harmonic generation. Upon analysis of 4D time-lapse images from the primary tumors, we found that inhibition of autocrine CSF1R led to a significant decrease in overall tumor cell motility in vivo (Figure 5A and Supplementary Movies 1–4). Acute inhibition of autocrine CSF1R signaling also led to decreased intravasation, as measured by multiphoton imaging of photoconverted tumor cells near flowing blood vessels (Figure 5B), as well as by count of circulating tumor cells in the blood (Figure 5C). Overall,

by both shRNA silencing as well as by antibody inhibition, our results indicate that autocrine CSF1R signaling is essential for tumor cell motility, invasion, intravasation and spontaneous lung metastasis in vivo.

Finally, we sought to test whether the CSF1R role in enhancing invasion was common to the claudin-low cell lines. We tested invasion in vitro in matrigel-coated chambers in the presence of TGFβ and the anti-human CSF1R inhibitory antibody. Interestingly, TGFβ stimulation alone did not increase basal invasion of MDA-MB-231 cells in this experiment, probably due to low treatment time (cells were exposed to TGFβ within invasion chambers overnight, while previously it had been used as a long pre-treatment before invasion assays [33]) (Figure 6A). However, CSF1R inhibition in the presence of TGFβ significantly decreased invasion in MDA-MB-231 cells (Figure 6A). We tested our panel of breast cancer cells for in vitro invasion in the same assay, and found that the luminal T47D and MCF7 cells showed minimal to no invasion in vitro (Figure 6B). However, when we tested the remaining cell lines, only the claudin-low cells showed a significant decrease in invasion in the presence of TGFβ and the inhibitory anti-CSF1R antibody similar to MDA-MB-231 (Figure 6C). In contrast, the basal-like MDA-MB-468 cells showed no significant change in invasion with either treatment (Figure 6C). The above data taken together show that autocrine CSF1R signaling enhances invasion and metastasis in claudin-low breast cancer cells in vitro and in vivo.

Autocrine CSF1R signaling attenuates expression of tight-junction proteins and maintains the “claudin-low” state

By closer observation of our intravital 4D movies, morphological differences between the primary tumors became apparent; control MDA-MB-231 cells were elongated and widely disconnected with each other, while CSF1R inhibition resulted to tumor cells that appeared more homogeneous, round and cohesive (Figure 5 and Supplemental Movies 1–4). Because CSF1R expression is higher in claudin-low patient tumors and cells lines (Figure 1), and because cohesiveness in epithelial cells is associated with expression of junction proteins (such as claudins), we hypothesized that autocrine CSF1R in breast tumor cells may be a regulator of claudins and other luminal proteins. In order to test this hypothesis, we analyzed the gene expression of MDA-MB-231 cells after inhibition of CSF1R signaling. We tested for standard markers used to characterize claudin-low tumors in the published literature (luminal keratins 8 and 19, as well as claudins 3, 4, 7 and occludin) [7]. We also tested for the atypical claudin 11, although very little is known about this protein in breast cancer, because a previous proteomics analysis showed potential interaction of claudin 11 with the activated CSF1R [34]. We found that mRNA expression of luminal keratins 8 and 19 (KRT8 and KRT19) as well as tight junction proteins claudin 4, 7, 11 and occludin (CLDN4, CLDN7, CLDN11 and OCLN) were significantly upregulated after CSF1R inhibition in vitro (Figure 7A). We confirmed this result in MDA-MB-231 cells by a second method, namely CSF1R knockdown by siRNA (Supplementary Figure 7A). We also confirmed that a similar overexpression of keratin 8 and claudins 3,4 and 7 was evident after CSF1R inhibition in a second claudin-low cell line, Hs578T (Supplementary Figure 7B). Moreover, we analyzed the gene expression of MDA-MB-231 tumors after CSF1R inhibition in vivo and found again a significant upregulation of luminal keratins and tight junction proteins (Figure 7B).

We validated the upregulation of several of these markers by western blot analysis in vitro (Figure 7C), and by immunohistochemistry of tumor tissue sections in vivo (Figure 7D). Similar to our observation from the intravital imaging (Figure 5 and Supplementary Movies 1–4), the immunohistochemical analysis also revealed that CSF1R–inhibited tumor cells appear in larger nests than the control tumor cells, suggesting that CSF1R inhibition may be associated with increased cohesion (Figure 7D). Our data indicate that autocrine CSF1R signaling suppresses gene expression of luminal keratins and tight junction proteins and is essential for maintaining the "claudin-low" state.

Finally, we sought to determine whether upregulation of these tight junction proteins was sufficient to recapitulate the phenotype of CSF1R inhibition: increased proliferation and decreased invasion. We generated stable MDA-MB-231 cells lines overexpressing the genes CLDN7, CLDN11 and OCLN (Supplementary Figure 8) and tested these cells for their proliferation and invasion properties in vitro, in the presence or absence of TGFβ as well as after CSF1R inhibition. MDA-MB-231 cells overexpressing CLDN7, CLDN11 and OCLN showed both a significant decrease in invasion through matrigel-coated transwells, as well as a significant increase in proliferation, as measured by EdU incorporation (Figure 7E). TGFβ stimulation or the inhibitory anti-CSF1R antibody alone had no significant effect in either of these processes (with the exception of occluding-overexpressing cells' proliferation) (Figure 7E). Inhibition of CSF1R in the presence of TGFβ similarly was not sufficient to reverse the abrogation of invasion; however, it significantly decreased proliferation in all overexpressing lines (Figure 3E). Such a proliferation decrease together with lack of invasion capacity was also evident in luminal cells (Figures 3C and 6B), suggesting that artificial overexpression of claudins in MDA-MB-231 forces them to resemble more the luminal T47D and MCF7 cells. Our data shows that increased expression of claudins is sufficient to recapitulate the main phenotypes of autocrine CSF1R inhibition into tipping the balance of breast cancer cells from invasion to proliferative growth.

DISCUSSION

In this study, we have assessed the role of autocrine CSF1R signaling in cancer progression of breast tumor cells. We show that TGFβ signaling upregulates expression of CSF1R specifically in claudin-low breast cancer cells, which in turn is essential for maintaining the "claudin-low" state; when CSF1R is inhibited, expression of luminal keratins and tight junction proteins is upregulated. The end phenotype of this autocrine CSF1R signaling determines the balance of the claudin-low tumor cells to either proliferate ("grow") or invade ("go"): when autocrine CSF1R signaling is present, junction proteins are suppressed and the balance is tipped over to invasion. In contrast, when autocrine CSF1R is inhibited, expression of junction proteins is released and the balance is tipped over to proliferation. A schematic for the proposed model of how autocrine CSF1R regulates progression in claudin-low breast tumor cells is shown in Figure 8.

Our in silico analysis of publicly available breast cancer patient microarray data [7] for mRNA levels of CSF1R and its ligand CSF1 showed that both are significantly higher in claudin-low tumors. A previously published analysis of older patient cohorts did not find a correlation for either CSF1 or CSF1R with tumor subtype, however claudin-low tumors

were not separated from basal-like tumors in those cohorts, therefore masking any differences in gene expression [31]. Despite both basal-like and claudin-low tumors being mostly triple-negative, claudin-low tumors show lesser expression of proliferation genes than basal-like tumors and are proposed to be slower-cycling tumors [7]. This could be partially explained by the findings presented in this study: autocrine CSF1R signaling attenuates proliferation in the presence of TGFβ specifically in claudin-low tumor cells, but not in basal-like tumor cells. More importantly, although the growth inhibitory effect of TGFβ in ER-negative breast cancer cells has been shown before, no previous report has shown a link for this phenotype to CSF1R signaling. We show here that autocrine CSF1R signaling is downstream of TGFβ, and essential both for the growth inhibitory effect, as well as the pro-invasive effect of TGFβ signaling in claudin-low breast tumor cells. Interestingly, these phenotypes were not evident in ER-positive tumor cells. How CSF1R is regulated specifically in claudin-low breast tumor cells but not in ER-positive cells is a study that is underway in our lab. Overall, this is the first study to link CSF1R signaling to the claudin-low breast cancer subtype and the first study to show that CSF1R is a main regulator of a "go or grow" switch in claudin-low breast cancer cells.

Moreover, we show here that autocrine CSF1R signaling is required for the maintenance of the claudin-low state in breast cancer cells, as inhibition of CSF1R leads to upregulation of claudins and occludin. TGFβ signaling has been previously shown to repress gene expression of claudins, mainly through the action of such transcription factors as Snail, Slug and Zeb1 [35–37]. This is the first study to show that CSF1R signaling is essential for this function and it is possible that these transcription factors can act downstream of autocrine CSF1R signaling. Interestingly, we found that overexpression of claudins was sufficient to lead to increased proliferation and decreased invasion in the MDA-MB-231 cells in vitro. The role of claudins in cancer progression is currently under intense investigation, with reports showing that they can act both as tumor suppressors and metastasis promoters [38]. Claudins 1, 3 and 4 have been shown to be associated with high grade and poor prognosis in gastric, colon and breast carcinoma [39–41], and claudin-1 overexpression leads to enlarged colon tumors in xenograft mice [41]. This agrees with our current study where overexpression of claudins 7, 11 and occludin led to increased cell proliferation. As far as metastasis is concerned, claudin-11 expression leads to decreased invasion in gastric cancer cells [42] and similarly we found here that overexpression of claudin 7, 11 and occludin leads to decreased invasion in MDA-MB-231 cells. It is possible that the opposite effect of claudins in proliferation versus invasion could account for their perceived role as both tumor suppressors and promoters. Of note, our report is the first study to show a role for claudin 11 in invasion and proliferation of breast cancer cells.

Overall, CSF1R has been shown to contribute to metastatic progression of breast cancer mainly through its role in tumor-associated macrophages [43, 44]. The main expectation for inhibition of CSF1R as a therapeutic target is that it will act on the macrophages in order to potentially revert them back to their normal function of attacking the tumor cells, enhance cytotoxic chemotherapeutic effects and potentially also block their metastasis-promoting functions [45]. However, tumor cells in patients also express CSF1R [23], and so far we have little information on how pharmaceutical inhibition would affect the tumor cells. We show here that inhibition of CSF1R can have very different effects in tumor cells of different

subtypes: while proliferation of luminal and basal-like cells was decreased, proliferation of claudin-low tumor cells was significantly increased. This suggests that CSF1R inhibition may have different results depending on the patient molecular subtype and that patients may need to be subdivided by subtype for such inhibitors to be tested efficiently in the clinic.

MATERIALS AND METHODS

Cell lines

MDA-MB-231, Hs578T, BT549, MCF7, T47D and MDA-MB-468 cells (ATCC, Manassas, VA) were cultured in DMEM with 10% fetal bovine serum (FBS), antibiotics (Invitrogen, Grand Island, NY) and insulin (Invitrogen) as suggested by ATCC. MDA-MB-231-GFP cells used to generate fluorescent tumors for intravital imaging were described previously [27].Knockdown and overexpressor MDA-MB-231 stable lines were generated by transduction with lentiviral particles purchased from the Einstein shRNA Core Facility. CSF1R shRNA sequences were RHS4430–101025591 and RHS4430–101031387 (Open Biosystems, Pittsburgh PA). Stable cell lines were selected with 10 μg/ml puromycin. A control cell line was generated with empty pGIPZ vector. Overexpression constructs were HsCD00434487 for CLDN7, PLOHS_100008613 for CLDN11 and PLOHS_100010097 for OCLN and vector encoding RFP as a control (Open Biosystems). Stable cell lines were selected with 10 μg/ml blasticidin.

Antibodies and siRNA

Inhibition experiments antibodies: anti-mouse CSF1R antibody (AFS98) [46], anti-human CSF1R antibody (MAB3291, R&D Systems, Minneapolis, MN). Western blot antibodies: anti-KRT8/18 (4546, Cell Signaling, Danvers, MA), anti-CLDN7 (34–9100, Invitrogen), anti-CLDN11 (ab53041, Abcam, Cambridge, MA), anti-OCLN (H00004950-M03A, Novus Biologicals, Littleton, CO). Immunohistochemistry: anti-cleaved caspace-3 (9661, Cell Signaling), anti-Iba1 (019–19741, Wako Chemicals, Richmond, VA), anti-Ki67 (VP-K451, Vector, Burlingame, CA), anti-BrdU (11170376001, Roche, New York, NY) and anti-KRT8 (ab107115, Abcam). siRNAs: CSF1R gene (M-003109-03–0005, Dharmacon, Pittsburgh PA), Smad3 gene (M-020067-00–0005, Dharmacon), both transfected by nucleofection as per the manufacturer's instructions (Lonza, Basel, Switzerland).

In vitro proliferation by EdU incorporation

200K cells were split into glass-bottom dishes (P35G-1.5–10-C, Mattek, Ashland, MA). Next day, 10 ng/ml TGFβ1 (100-B-001/CF, R&D Systems), control IgG or inhibitory anti-human CSF1R antibody (10 μg/ml) were added for 24 hours. Staining for EdU was performed with the Click-iT EdU Alexa Fluo 488 kit as per the manufacturer's instructions (C10350, Invitrogen). Nuclei were counterstained with DAPI. Samples were imaged at ×40 magnification with an Inverted Olympus IX70 microscope (at least 15 random images per dish, three different experiments with duplicate dishes each). Processing and quantification was performed in ImageJ. Results were calculated as percentage of EdU-positive nuclei over total.

Transwell invasion assay

Invasion was evaluated as described previously [47]. 10 ng/ml TGFβ1, control IgG or inhibitory anti-human CSF1R antibody (10 μg/ml) were added in both the upper and bottom chambers.

Westen Blot

MDA-MB-231 cells were treated in vitro with either control IgG or inhibitory anti-human CSF1R antibody (50 μg/ml) in complete media for 48 hours, after which they were lyzed and assayed by western blot as previously described [47].

RNA extraction and PCR

RNA extraction from cultured cells and from primary tumor cells (>95% pure tumor cell population by FACS), reverse transcription and amplification was performed as previously described [27, 48]. Gene-specific primer sequences are shown in the Supplementary Table.

Mouse Xenograft Model

All procedures were conducted in accordance with the National Institutes of Health regulations, and approved by the Einstein animal care committee. A total of 2×10^6 MDA-MB-231 cells (parental, expressing GFP [27], vector control, or CSF1R shRNA knockdown cells) per animal were suspended in sterile PBS with 20% collagen I (BD Biosciences) and injected into the lower left mammary gland of SCID mice (NCI, Frederick, MD). Tumor growth for the knockdown cell lines was measured at 9 weeks post-injection according to the formula $V=W^2 \times L/2$ (W: width, L: length). All other experiments were performed on tumors that were 1–1.2 cm in diameter. For treatments with the blocking antibodies, mice were injected intraperitoneally twice at 48 and 24 hours prior to experiments. For histology and immunostaining experiments, primary tumors were excised, fixed in formalin, and paraffin embedded. Sections from the middle of the primary tumors were stained with hematoxylin and eosin (H&E) for general histology, or immunostained with specific antibodies, as described previously [47, 48]. Necrotic tumor areas were excluded from the analysis (no significant difference in overall necrosis was seen between cell lines).

In vivo invasion assay

Cell collection of invasive cells from primary tumors was performed as previously described [27, 48, 49].

Intravasation assay

The number of circulating tumor cells in the peripheral blood of tumor-bearing mice was performed as previously described [48, 50].

Lung metastasis assays

Spontaneous lung metastases and experimental lung metastasis in MDA-MB-231 xenografts were performed as previously described [47].

Intravital Imaging

Intravital imaging was performed as described in [18]. Briefly, orthotopic tumors of MDA-MB-231-GFP cells at 0.8–1cm diameter were exposed by skin flap surgery on anesthetized mice, and imaging was performed using an Olympus FV1000-MPE multiphoton system with 880nm excitation. We imaged random fields of 512×512 μm at 512×512 pixels for a depth of 100 μm (21 slices at 5 μm steps) beginning at the edge of the tumor for a total of 30 min (2 min intervals). Images were reconstructed in 4D using ImageJ. For the in vivo intravasation assay, the mammary imaging window implantation and photoconversion were performed as described previously [51, 52]. Photoconversion sites were chosen in areas containing at least one flowing blood vessel. Imaging of the photoconverted areas at 0 and 24 hours was performed using a custom-built multiphoton system [53]. Imaging and quantification on ImageJ was performed as described previously [51].

Analysis of breast cancer cohort microarray data

For the UNC337 cohort, gene expression and clinical data published in [7] were downloaded from the UNC Microarray Database (https://genome.unc.edu). Gene expression data for CSF1 and CSF1R were extracted and grouped by molecular subtype as annotated in the accompanying clinical patient datasheet. Plots and statistical analysis were generated in GraphPad Prism 6.

Supplementary Material

Refer to Web version on PubMed Central for supplementary material.

ACKNOWLEDGEMENTS

We thank Drs. Paraic Kenny, Richard Stanley, Jeffrey Segall and members of the Condeelis lab for helpful discussions. The AFS98, total and phospho-Y559 CSF1R antibodies were a generous gift from Dr. Richard Stanley. For technical help at Albert Einstein College of Medicine, we thank the Histotechnology and Comparative Pathology Facility, the shRNA Core Facility, the FACS Facility (supported by NCI P30 CA 013330) and the Genomics Facility. This work was supported by NCI grants 5RO1CA164468 (AP, YW, XC, DE, JC) and RO1CA170507 (JP, MO, JC).

REFERENCES

1. Perou CM, Sorlie T, Eisen MB, van de Rijn M, Jeffrey SS, Rees CA, et al. Molecular portraits of human breast tumours. Nature. 2000; 406:747–752. [PubMed: 10963602]
2. Sorlie T, Perou CM, Tibshirani R, Aas T, Geisler S, Johnsen H, et al. Gene expression patterns of breast carcinomas distinguish tumor subclasses with clinical implications. Proc Natl Acad Sci U S A. 2001; 98:10869–10874. [PubMed: 11553815]
3. Sorlie T, Tibshirani R, Parker J, Hastie T, Marron JS, Nobel A, et al. Repeated observation of breast tumor subtypes in independent gene expression data sets. Proc Natl Acad Sci U S A. 2003; 100:8418–8423. [PubMed: 12829800]
4. Sotiriou C, Neo SY, McShane LM, Korn EL, Long PM, Jazaeri A, et al. Breast cancer classification and prognosis based on gene expression profiles from a population-based study. Proc Natl Acad Sci U S A. 2003; 100:10393–10398. [PubMed: 12917485]
5. Hu Z, Fan C, Oh DS, Marron JS, He X, Qaqish BF, et al. The molecular portraits of breast tumors are conserved across microarray platforms. BMC genomics. 2006; 7:96. [PubMed: 16643655]

6. Herschkowitz JI, Simin K, Weigman VJ, Mikaelian I, Usary J, Hu Z, et al. Identification of conserved gene expression features between murine mammary carcinoma models and human breast tumors. Genome Biol. 2007; 8:R76. [PubMed: 17493263]
7. Prat A, Parker JS, Karginova O, Fan C, Livasy C, Herschkowitz JI, et al. Phenotypic and molecular characterization of the claudin-low intrinsic subtype of breast cancer. Breast Cancer Res. 2010; 12:R68. [PubMed: 20813035]
8. Sotiriou C, Pusztai L. Gene-expression signatures in breast cancer. N Engl J Med. 2009; 360:790–800. [PubMed: 19228622]
9. Weigelt B, Pusztai L, Ashworth A, Reis-Filho JS. Challenges translating breast cancer gene signatures into the clinic. Nature reviews Clinical oncology. 2012; 9:58–64.
10. Kacinski BM, Carter D, Mittal K, Kohorn EI, Bloodgood RS, Donahue J, et al. High level expression of fms proto-oncogene mRNA is observed in clinically aggressive human endometrial adenocarcinomas. Int J Radiat Oncol Biol Phys. 1988; 15:823–829. [PubMed: 3182322]
11. Kacinski BM, Carter D, Mittal K, Yee LD, Scata KA, Donofrio L, et al. Ovarian adenocarcinomas express fms-complementary transcripts and fms antigen, often with coexpression of CSF-1. Am J Pathol. 1990; 137:135–147. [PubMed: 1695482]
12. Kacinski BM, Scata KA, Carter D, Yee LD, Sapi E, King BL, et al. FMS (CSF-1 receptor) and CSF-1 transcripts and protein are expressed by human breast carcinomas in vivo and in vitro. Oncogene. 1991; 6:941–952. [PubMed: 1829808]
13. Scholl SM, Lidereau R, de la Rochefordiere A, Le-Nir CC, Mosseri V, Nogues C, et al. Circulating levels of the macrophage colony stimulating factor CSF-1 in primary and metastatic breast cancer patients. A pilot study. Breast Cancer Res Treat. 1996; 39:275–283. [PubMed: 8877007]
14. Kacinski BM, Stanley ER, Carter D, Chambers JT, Chambers SK, Kohorn EI, et al. Circulating levels of CSF-1 (M-CSF) a lymphohematopoietic cytokine may be a useful marker of disease status in patients with malignant ovarian neoplasms. Int J Radiat Oncol Biol Phys. 1989; 17:159–164. [PubMed: 2663797]
15. Scholl SM, Bascou CH, Mosseri V, Olivares R, Magdelenat H, Dorval T, et al. Circulating levels of colony-stimulating factor 1 as a prognostic indicator in 82 patients with epithelial ovarian cancer. Br J Cancer. 1994; 69:342–346. [PubMed: 8297732]
16. Wyckoff J, Wang W, Lin EY, Wang Y, Pixley F, Stanley ER, et al. A paracrine loop between tumor cells and macrophages is required for tumor cell migration in mammary tumors. Cancer Res. 2004; 64:7022–7029. [PubMed: 15466195]
17. Roussos ET, Balsamo M, Alford SK, Wyckoff JB, Gligorijevic B, Wang Y, et al. Mena invasive (MenaINV) promotes multicellular streaming motility and transendothelial migration in a mouse model of breast cancer. J Cell Sci. 2011; 124:2120–2131. [PubMed: 21670198]
18. Patsialou A, Bravo-Cordero JJ, Wang Y, D E, Liu H, Clarke M, et al. Intravital multiphoton imaging reveals multicellular streaming as a crucial component of in vivo cell migration in human breast tumors. IntraVital. 2013; 2:e25294. [PubMed: 25013744]
19. Lin EY, Nguyen AV, Russell RG, Pollard JW. Colony-stimulating factor 1 promotes progression of mammary tumors to malignancy. J Exp Med. 2001; 193:727–740. [PubMed: 11257139]
20. Aharinejad S, Paulus P, Sioud M, Hofmann M, Zins K, Schafer R, et al. Colony-stimulating factor-1 blockade by antisense oligonucleotides and small interfering RNAs suppresses growth of human mammary tumor xenografts in mice. Cancer Res. 2004; 64:5378–5384. [PubMed: 15289345]
21. Paulus P, Stanley ER, Schafer R, Abraham D, Aharinejad S. Colony-stimulating factor-1 antibody reverses chemoresistance in human MCF-7 breast cancer xenografts. Cancer Res. 2006; 66:4349–4356. [PubMed: 16618760]
22. DeNardo DG, Brennan DJ, Rexhepaj E, Ruffell B, Shiao SL, Madden SF, et al. Leukocyte complexity predicts breast cancer survival and functionally regulates response to chemotherapy. Cancer discovery. 2011; 1:54–67. [PubMed: 22039576]
23. Kacinski BM. CSF-1 and its receptor in breast carcinomas and neoplasms of the female reproductive tract. Mol Reprod Dev. 1997; 46:71–74. [PubMed: 8981366]

24. Filderman AE, Bruckner A, Kacinski BM, Deng N, Remold HG. Macrophage colony-stimulating factor (CSF-1) enhances invasiveness in CSF-1 receptor-positive carcinoma cell lines. Cancer Res. 1992; 52:3661–3666. [PubMed: 1535551]
25. Sapi E, Flick MB, Rodov S, Gilmore-Hebert M, Kelley M, Rockwell S, et al. Independent regulation of invasion and anchorage-independent growth by different autophosphorylation sites of the macrophage colony-stimulating factor 1 receptor. Cancer Res. 1996; 56:5704–5712. [PubMed: 8971179]
26. Wrobel CN, Debnath J, Lin E, Beausoleil S, Roussel MF, Brugge JS. Autocrine CSF-1R activation promotes Src-dependent disruption of mammary epithelial architecture. J Cell Biol. 2004; 165:263–273. [PubMed: 15117969]
27. Patsialou A, Wyckoff J, Wang Y, Goswami S, Stanley ER, Condeelis JS. Invasion of human breast cancer cells in vivo requires both paracrine and autocrine loops involving the colony-stimulating factor-1 receptor. Cancer Res. 2009; 69:9498–9506. [PubMed: 19934330]
28. Taube JH, Herschkowitz JI, Komurov K, Zhou AY, Gupta S, Yang J, et al. Core epithelial-to-mesenchymal transition interactome gene-expression signature is associated with claudin-low and metaplastic breast cancer subtypes. Proc Natl Acad Sci U S A. 2010; 107:15449–15454. [PubMed: 20713713]
29. Arteaga CL, Tandon AK, Von Hoff DD, Osborne CK. Transforming growth factor beta: potential autocrine growth inhibitor of estrogen receptor-negative human breast cancer cells. Cancer Res. 1988; 48:3898–3904. [PubMed: 3164252]
30. Zugmaier G, Ennis BW, Deschauer B, Katz D, Knabbe C, Wilding G, et al. Transforming growth factors type beta 1 and beta 2 are equipotent growth inhibitors of human breast cancer cell lines. J Cell Physiol. 1989; 141:353–361. [PubMed: 2808542]
31. Morandi A, Barbetti V, Riverso M, Dello Sbarba P, Rovida E. The colony-stimulating factor-1 (CSF-1) receptor sustains ERK1/2 activation and proliferation in breast cancer cell lines. PloS one. 2011; 6:e27450. [PubMed: 22096574]
32. Qian BZ, Pollard JW. Macrophage diversity enhances tumor progression and metastasis. Cell. 2010; 141:39–51. [PubMed: 20371344]
33. Farina AR, Coppa A, Tiberio A, Tacconelli A, Turco A, Colletta G, et al. Transforming growth factor-beta1 enhances the invasiveness of human MDA-MB-231 breast cancer cells by up-regulating urokinase activity. Int J Cancer. 1998; 75:721–730. [PubMed: 9495240]
34. Cross M, Nguyen T, Bogdanoska V, Reynolds E, Hamilton JA. A proteomics strategy for the enrichment of receptor-associated complexes. Proteomics. 2005; 5:4754–4763. [PubMed: 16267818]
35. Ikenouchi J, Matsuda M, Furuse M, Tsukita S. Regulation of tight junctions during the epithelium-mesenchyme transition: direct repression of the gene expression of claudins/occludin by Snail. J Cell Sci. 2003; 116:1959–1967. [PubMed: 12668723]
36. Martinez-Estrada OM, Culleres A, Soriano FX, Peinado H, Bolos V, Martinez FO, et al. The transcription factors Slug and Snail act as repressors of Claudin-1 expression in epithelial cells. Biochem J. 2006; 394:449–457. [PubMed: 16232121]
37. Aigner K, Dampier B, Descovich L, Mikula M, Sultan A, Schreiber M, et al. The transcription factor ZEB1 (deltaEF1) promotes tumour cell dedifferentiation by repressing master regulators of epithelial polarity. Oncogene. 2007; 26:6979–6988. [PubMed: 17486063]
38. Myal Y, Leygue E, Blanchard AA. Claudin 1 in breast tumorigenesis: revelation of a possible novel “claudin high” subset of breast cancers. Journal of biomedicine & biotechnology. 2010; 2010:956897. [PubMed: 20490282]
39. Lanigan F, McKiernan E, Brennan DJ, Hegarty S, Millikan RC, McBryan J, et al. Increased claudin-4 expression is associated with poor prognosis and high tumour grade in breast cancer. Int J Cancer. 2009; 124:2088–2097. [PubMed: 19142967]
40. Resnick MB, Gavilanez M, Newton E, Konkin T, Bhattacharya B, Britt DE, et al. Claudin expression in gastric adenocarcinomas: a tissue microarray study with prognostic correlation. Hum Pathol. 2005; 36:886–892. [PubMed: 16112005]

41. Dhawan P, Singh AB, Deane NG, No Y, Shiou SR, Schmidt C, et al. Claudin-1 regulates cellular transformation and metastatic behavior in colon cancer. J Clin Invest. 2005; 115:1765–1776. [PubMed: 15965503]
42. Agarwal R, Mori Y, Cheng Y, Jin Z, Olaru AV, Hamilton JP, et al. Silencing of claudin-11 is associated with increased invasiveness of gastric cancer cells. PloS one. 2009; 4:e8002. [PubMed: 19956721]
43. Condeelis J, Pollard JW. Macrophages: obligate partners for tumor cell migration, invasion, and metastasis. Cell. 2006; 124:263–266. [PubMed: 16439202]
44. Pollard JW. Macrophages define the invasive microenvironment in breast cancer. J Leukoc Biol. 2008; 84:623–630. [PubMed: 18467655]
45. Ruffell B, Affara NI, Coussens LM. Differential macrophage programming in the tumor microenvironment. Trends Immunol. 2012; 33:119–126. [PubMed: 22277903]
46. Sudo T, Nishikawa S, Ogawa M, Kataoka H, Ohno N, Izawa A, et al. Functional hierarchy of c-kit and c-fms in intramarrow production of CFU-M. Oncogene. 1995; 11:2469–2476. [PubMed: 8545103]
47. Gil-Henn H, Patsialou A, Wang Y, Warren MS, Condeelis JS, Koleske AJ. Arg/Abl2 promotes invasion and attenuates proliferation of breast cancer in vivo. Oncogene. 2013; 32:2622–2630. [PubMed: 22777352]
48. Patsialou A, Wang Y, Lin J, Whitney K, Goswami S, Kenny PA, et al. Selective gene-expression profiling of migratory tumor cells in vivo predicts clinical outcome in breast cancer patients. Breast Cancer Res. 2012; 14:R139. [PubMed: 23113900]
49. Wyckoff JB, Segall JE, Condeelis JS. The collection of the motile population of cells from a living tumor. Cancer research. 2000; 60:5401–5404. [PubMed: 11034079]
50. Wyckoff JB, Jones JG, Condeelis JS, Segall JE. A critical step in metastasis: in vivo analysis of intravasation at the primary tumor. Cancer Res. 2000; 60:2504–2511. [PubMed: 10811132]
51. Gligorijevic B, Wyckoff J, Yamaguchi H, Wang Y, Roussos ET, Condeelis J. N-WASP-mediated invadopodium formation is involved in intravasation and lung metastasis of mammary tumors. J Cell Sci. 2012; 125:724–734. [PubMed: 22389406]
52. Kedrin D, Gligorijevic B, Wyckoff J, Verkhusha VV, Condeelis J, Segall JE, et al. Intravital imaging of metastatic behavior through a mammary imaging window. Nat Methods. 2008; 5:1019–1021. [PubMed: 18997781]
53. Entenberg D, Wyckoff J, Gligorijevic B, Roussos ET, Verkhusha VV, Pollard JW, et al. Setup and use of a two-laser multiphoton microscope for multichannel intravital fluorescence imaging. Nat Protoc. 2011; 6:1500–1520. [PubMed: 21959234]

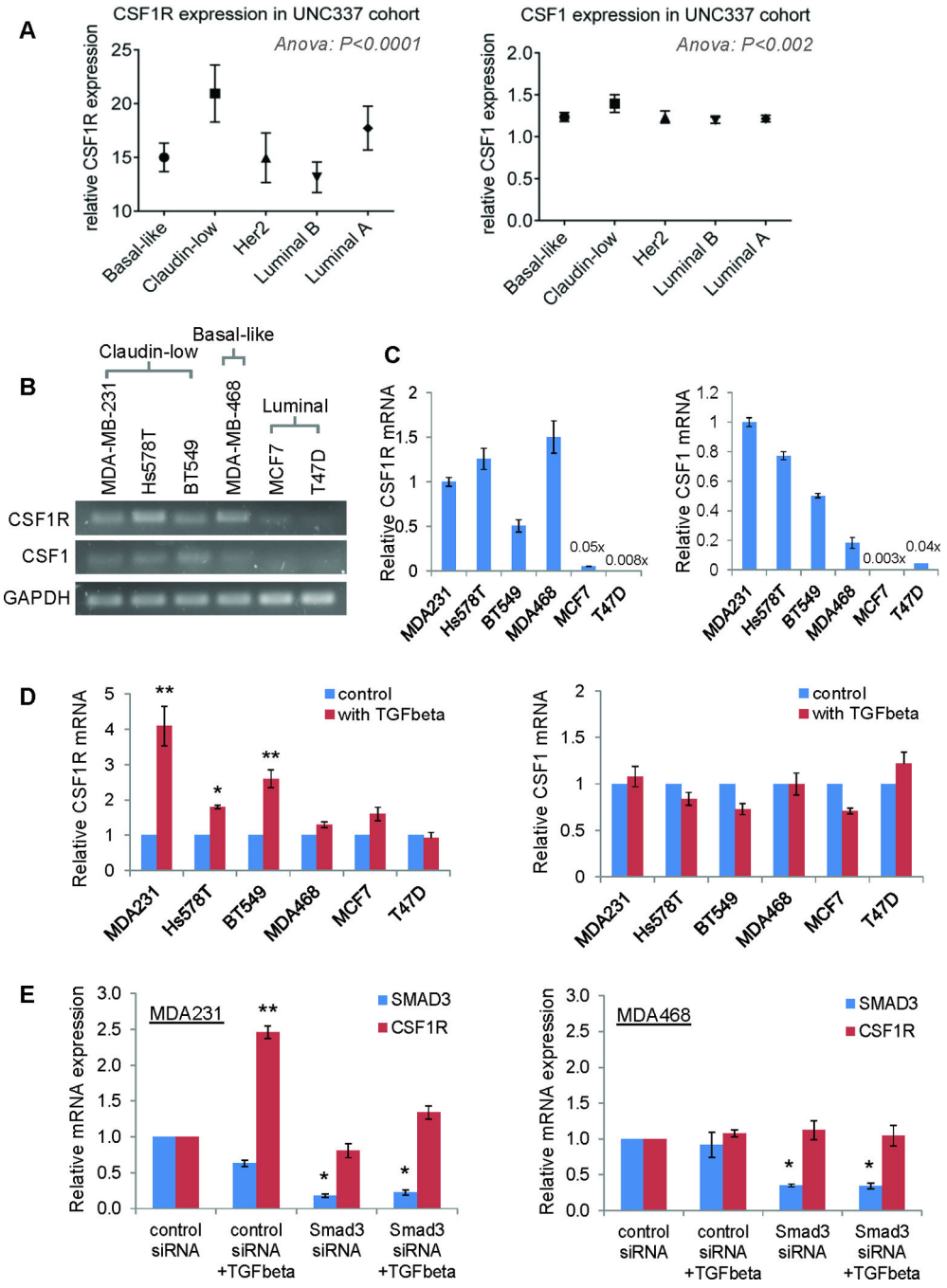

Figure 1. Claudin-low breast tumor cells have higher expression of CSF1R that is regulated by TGFβ

A. Expression of CSF1R and its ligand, CSF1, were examined in the UNC337 breast cancer cohort. The average relative CSF1R or CSF1 expression is plotted by molecular subtype. Analysis of variance was measured between groups by Anova. Error bars: 95% CI (confidence interval).

B. mRNA expression of CSF1 and CSF1R was assessed in a panel of breast cancer cell lines by PCR and agarose gel electrophoresis. Shown is a representative image from 3 separate experiments. GAPDH was used as a positive control.

C. mRNA expression levels for CSF1 and CSF1R in the various breast cancer cells lines were quantitatively evaluated by real-time PCR. Results are plotted as the average relative mRNA expression for each cell line normalized to MDA-MB-231 cells. N=3 separate experiments with 2 technical repeats per experiment.

D. mRNA expression for CSF1 and CSF1R was assessed in the presence or absence of TGFβ1 stimulation. Results are plotted as a fold ratio for each cell line relative to the control. N=3 separate experiments with 2 technical repeats per experiment.

E. mRNA expression for CSF1R was assessed in the presence or absence of TGFβ1, after transfection with either a control scrambled siRNA sequence or siRNA towards the Smad3 gene. Results are plotted as a fold ratio for each cell line and its gene relative to its control. Data is presented for MDA-MB-231 cells and for MDA-MB-468 cells. N=3 separate biological experiments per cell line.

Error bars: Mean ± SEM. *: $p<0.05$, **: $p<0.01$ (by Student's t-test).

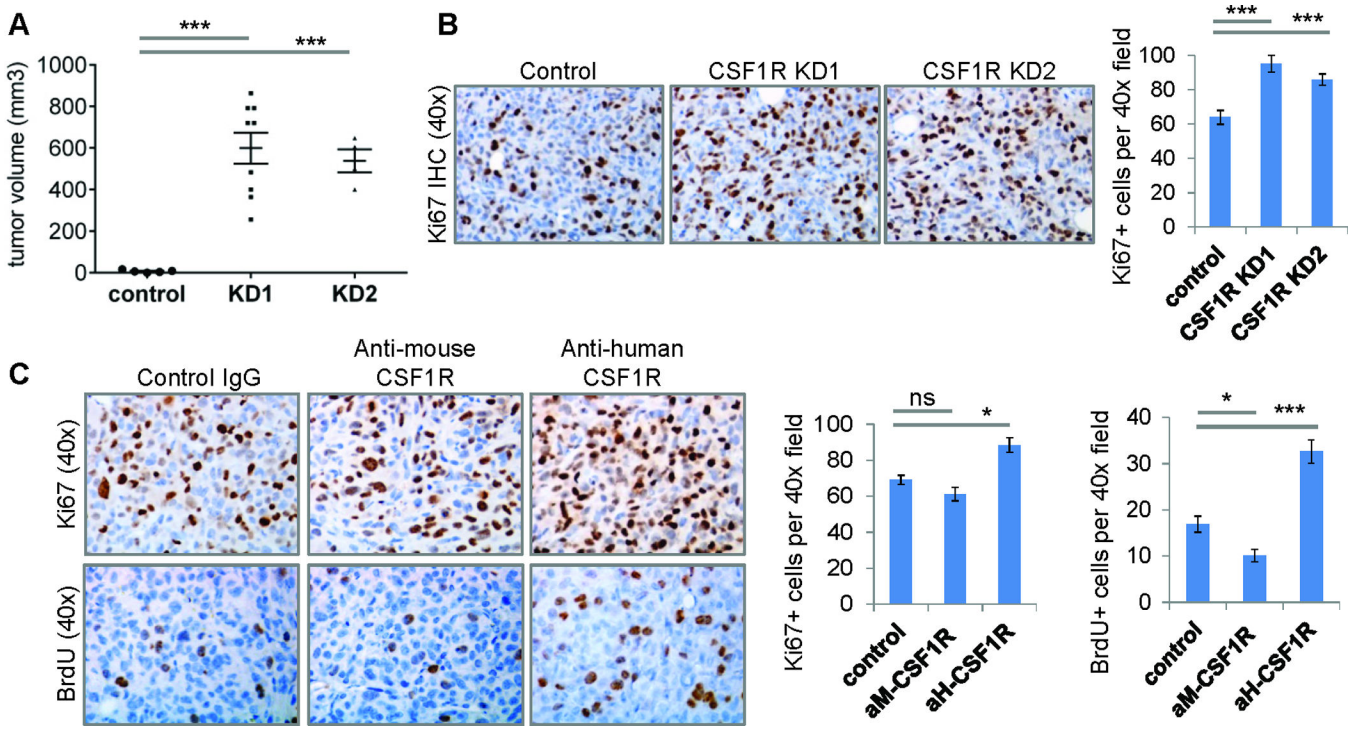

Figure 2. Inhibition of autocrine CSF1R signaling in vivo leads to enlarged primary tumors due to increased proliferation

A. Orthotopic xenograft tumors were generated with MDA-MB-231 cells, stably expressing either control vector or CSF1R shRNA (KD1 and KD2 for two different shRNA sequences). Tumor size was measured at 9 weeks post-injection and shown in the scatter plot. N=5 mice for control, 9 mice for KD1 and 5 mice for KD2.

B. Representative images and quantification of proliferating cells in the control, KD1 and KD2 tumors by ki7 immunohistochemical staining. Results are shown as the average number of ki67-positive cells per 40x field imaged. N=3 tumors per condition.

C. Representative images and quantification of proliferating cells in parental MDA-MB-231 tumors, treated with either control IgG or inhibitory antibodies to mouse (aM-CSF1R) or human CSF1R (aH-CSF1R). Proliferating cells were assessed by immunohistochemistry for ki67 and BrdU. Results are shown as the average number of ki67-positive cells or BrdU-positive cells per 40x field imaged. N=3 tumors per condition.

Error bars: Mean ± SEM. *: $p<0.05$, ***: $p<0.001$, ns: not significant (by Student's t-test).

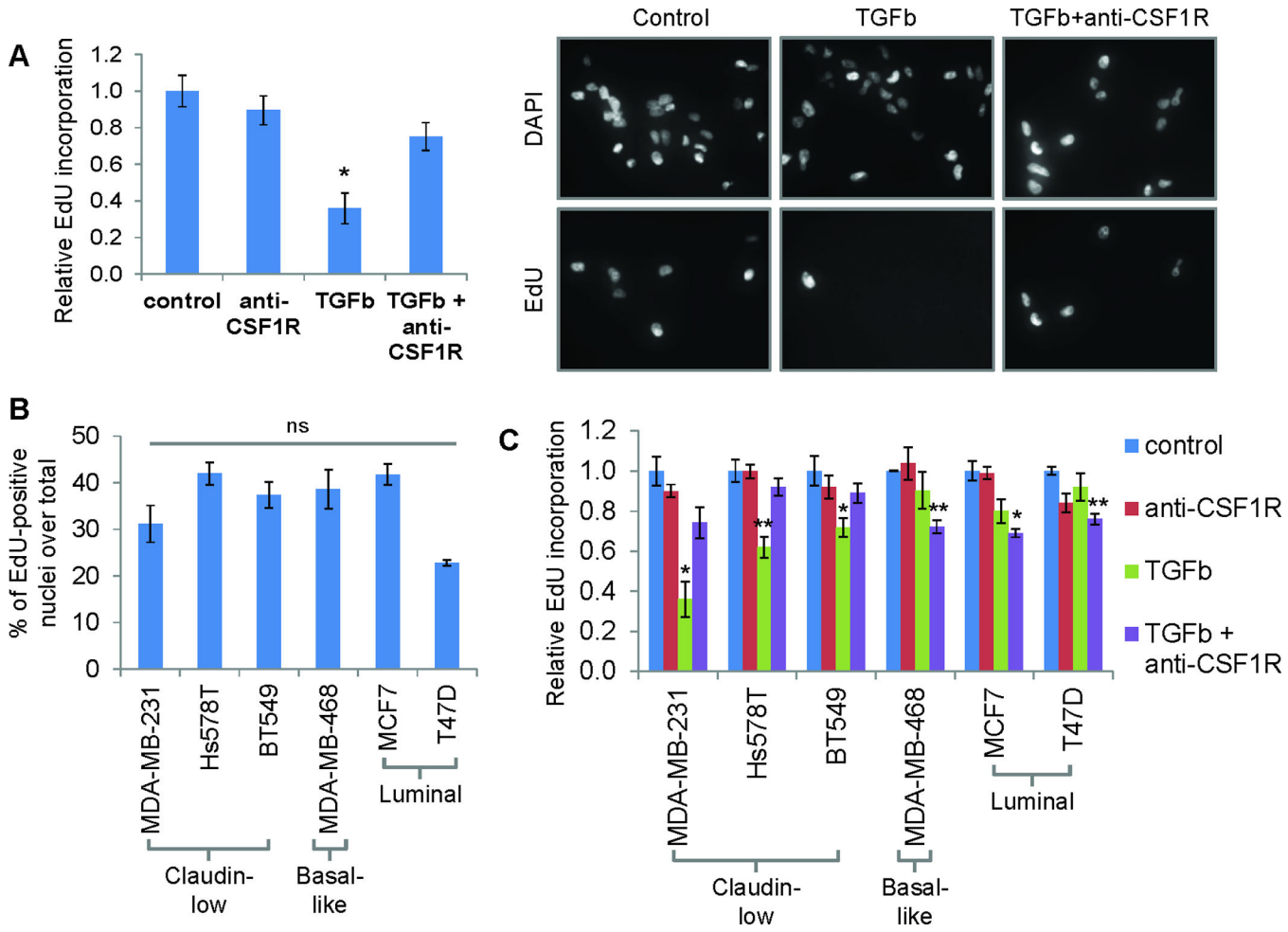

Figure 3. Autocrine CSF1R is required in claudin-low breast tumor cells to maintain growth inhibition downstream of TGFβ

A. MDA-MB-231 cells in vitro were treated with either TGFβ, an inhibitory antibody to human CSF1R (anti-CSF1R) or both for 24 hours, and subsequently assayed for S-phase cell cycle progression by EdU incorporation. Results are plotted as the relative amount of EdU-positive nuclei per total (stained by DAPI) normalized to control. Representative images are shown at 40x magnification.

B. Relative proliferation rates between the breast cancer cell lines. Proliferation rates were measured by EdU incorporation as shown in panel A. Statistical tests were performed for all cell lines compared to MDA-MB-231.

C. In vitro proliferation by EdU incorporation was measured in the various breast cancer cell lines, treated with either TGFβ, the inhibitory antibody to human CSF1R or both, similar to panel A. Results are shown as relative EdU incorporation normalized to each cell line's control condition. Data for MDA-MB-231 cells are repeated here from panel A for ease of comparison.

N=3 separate experiments with duplicates plates. Error bars: Mean ± SEM. *: $p<0.05$, **: $p<0.01$, ns: not significant (by Student's t-test).

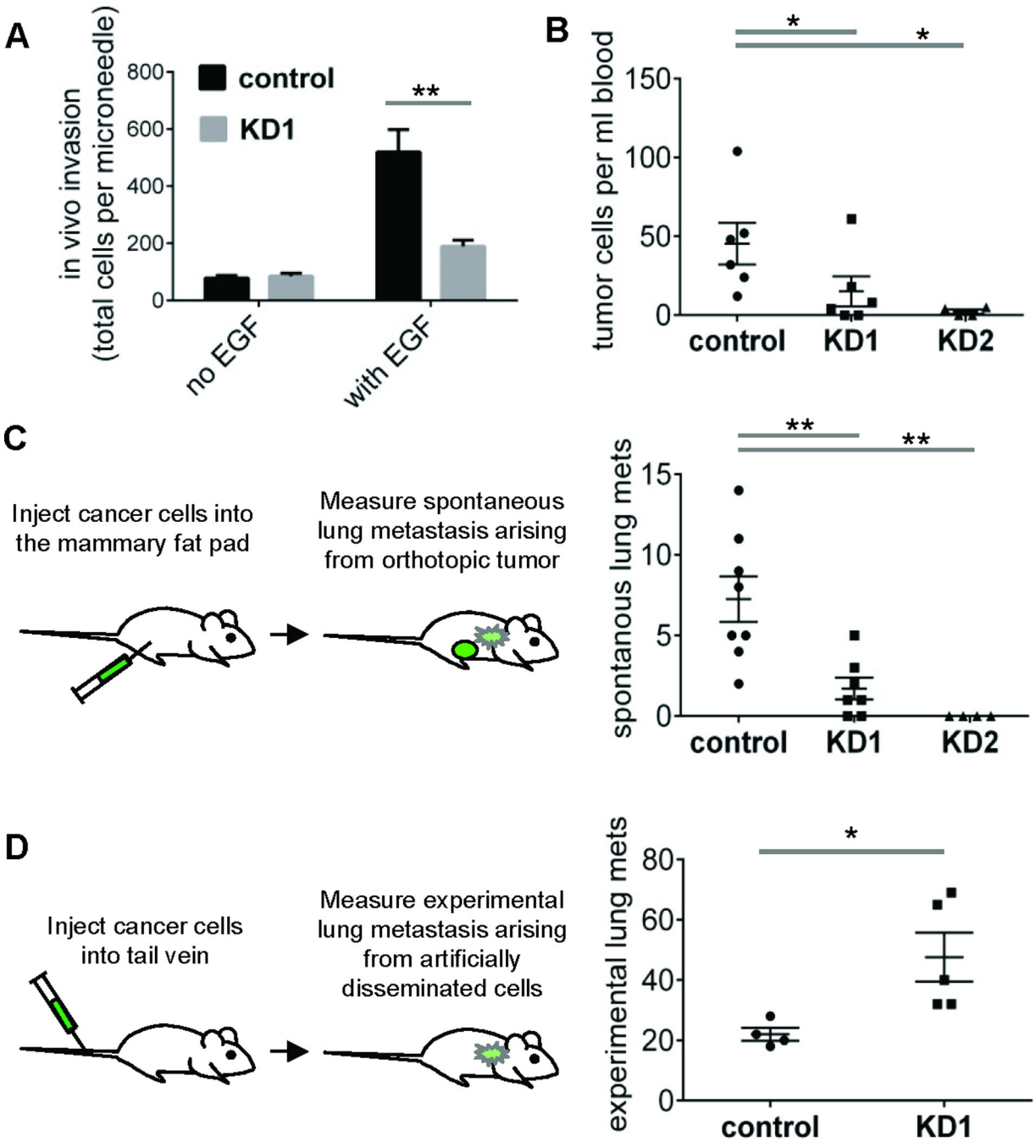

Figure 4. Knockdown of CSF1R in primary breast tumors leads to decreased invasion, intravasation and lung metastasis in vivo

A. In vivo invasion towards EGF was measured in orthotopic tumors generated with either control or CSF1R knockdown KD1 MDA-MB-231 cells. Total cells were counted by DAPI staining. N=4 mice per condition.

B. Intravasation was measured as total circulating tumor cells per ml of peripheral blood in mice bearing equal diameter orthotopic tumors of either control, KD1 or KD2 cells. N=7 mice for control, 7 mice for KD1 and 5 mice for KD2 tumors.

C. Quantification of spontaneous lung metastasis by histological examination of metastatic colonies in lung tissue from orthotopic tumors generated with either control, KD1 or KD2 cells. N=8 mice for control, 7 mice for KD1 and 5 mice for KD2 tumors.
D. Quantification of experimental lung metastasis by histological examination of metastatic colonies at 4 weeks following tail vein injection of equal numbers of control or KD1 cells to mice. N=5 mice per condition.
Error bars: Mean ± SEM. *: $p<0.05$, **: $p<0.01$ (by Student's t-test).

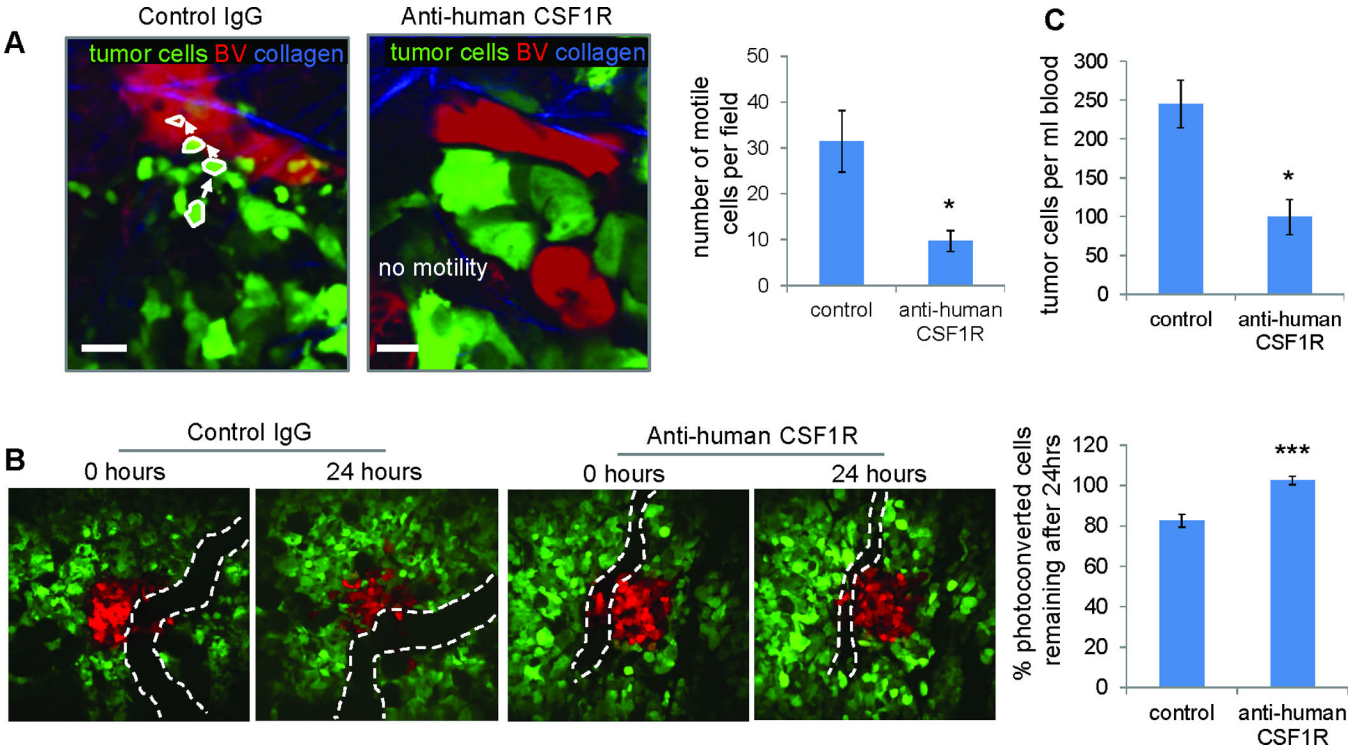

Figure 5. Intravital multiphoton imaging reveals decreased tumor cell motility and intravasation upon CSF1R inhibition in vivo

A. Representative images and quantification of in vivo tumor cell motility in parental MDA-MB-231 orthotopic tumors treated with either control IgG or the inhibitory antibody to human CSF1R. In the still images shown here (extracted from Supplementary Movies 1 and 3), tumor cells are green (due to stable GFP expression in the MDA-MB-231 cells), blood vessels are red (due to intravenous injection of Texas-red dextran in the mice prior to the imaging session) and collagen fibers are blue (due to second harmonic generation). In the left image, motile cells are outlined in white and arrows denote the direction of movement for the motile cells. The right image showed no motility. Quantification is shown as average number of motile cells per field. Scale bar: 20 μm. N=8 mice for control, 5 mice for anti-mouse CSF1R and 6 mice for anti-human CSF1R.

B. In vivo intravasation was measured in orthotopic MDA-MB-231 tumors by intravital multiphoton microscopy through a mammary imaging window. At 0 hours, cells were photoconverted (red) in an area containing flowing blood vessels. Then tumors were treated with either control IgG or an inhibitory antibody to the human CSF1R and the same area was imaged again 24 hours later. Images are shown at 25x magnification. Quantification is shown as percentage of red tumor cells remaining around blood vessels at 24 hours relative to the 0 hour timepoint. N=4 mice for control, 5 mice for anti-CSF1R treatment, with 3–5 different areas imaged per mouse. Error bars: Mean ± SEM. ***: $p<0.001$ (by Student's t-test).

C. Intravasation measured as total circulating tumor cells per ml of peripheral blood in mice bearing parental MDA-MB-231 tumors and treated with control IgG or the inhibitory antibody to human CSF1R. N= 6 mice for control, 16 mice for the anti-CSF1R treatment. Error bars: Mean ± SEM. *: $p<0.05$, ns: not significant (by Student's t-test).

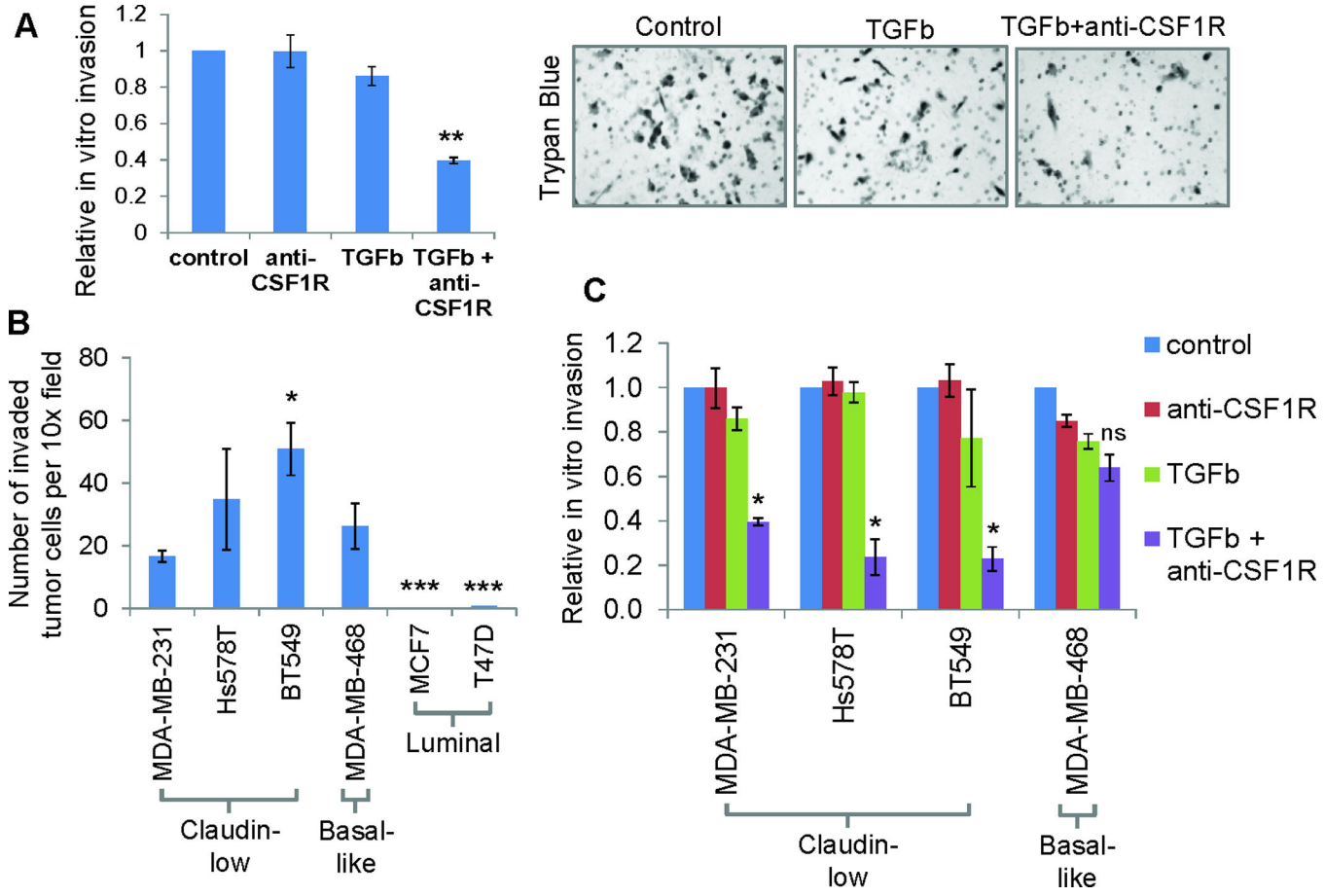

Figure 6. Inhibition of CSF1R signaling in vitro leads to decreased invasion in claudin-low breast tumor cells

A. MDA-MB-231 cells were plated on matrigel-coated transwells in the presence of either TGFβ1, an inhibitory antibody to the human CSF1R (anti-CSF1R) or both, and allowed to invade for 24 hours. Results are shown as the relative number of cells imaged at the bottom side of the transwells after 24 hours normalized to control. Representative images of the bottom side of the transwell filters used for the quantification are shown at 10x magnification.

B. Relative invasion properties between the breast cancer cell lines. Results are plotted as number or cells invaded per 10x field imaged. Note that MCF7 and T47D showed minimal invasion, with 1–2 invaded cells counted in only one technical repeat of one experiment from total 3 different experiments. Statistical tests were performed for all cell lines compared to MDA-MB-231.

C. In vitro invasion was measured in the various breast cancer cell lines, treated with either TGFβ1, the inhibitory antibody to the human CSF1R or both, similar to panel A. MCF7 and T47D were omitted due to minimal basal invasion. Results are shown as average numbers of invaded cells normalized to each cell line's control condition. Data for MDA-MB-231 cells are repeated here from panel A for ease of comparison.

N= 3 separate experiments with duplicate transwells. Error bars: Mean ± SEM. *: $p<0.05$, **: $p<0.01$, ***: $p<0.001$, ns: not significant (by Student's t-test).

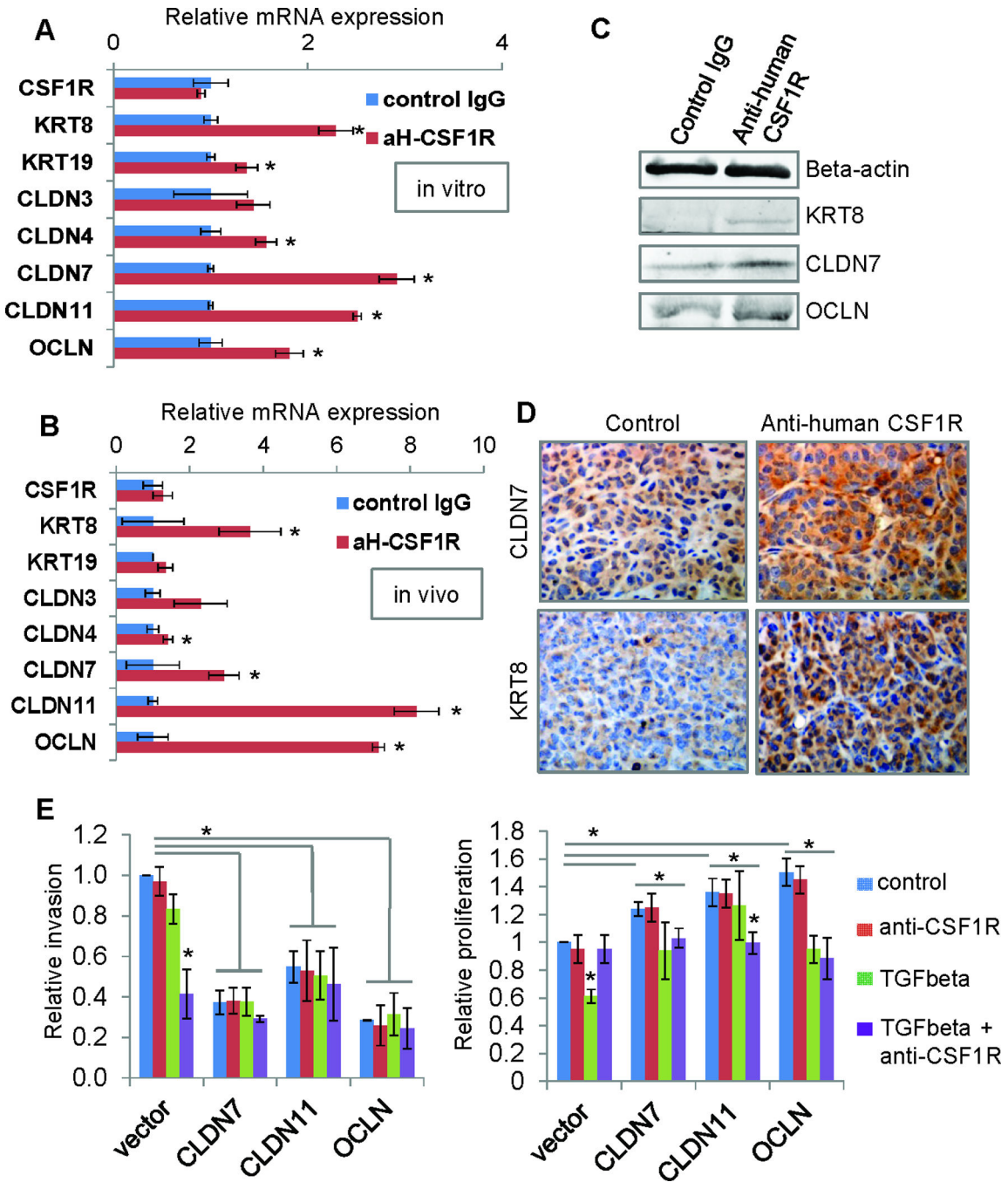

Figure 7. Autocrine CSF1R signaling maintains low expression of tight junction proteins and luminal keratins in claudin-low breast cancer cells

A. MDA-MB-231 cells were treated in vitro with either control or the inhibitory antibody to human CSF1R (aH-CSF1R), in the presence of TGFβ. After 48hours, mRNA expression of a panel of luminal keratins and tight junction proteins was assessed by real-time PCR. Results are shown as average mRNA expression relative to control treatment. N=3 separate experiments with duplicate plates.

B. MDA-MB-231 orthotopic tumors were treated in vivo with either control IgG or the inhibitory antibody to human CSF1R (aH-CSF1R). After 48hours, tumor cells were isolated

by FACS (due to GFP stable expression in the MDA-MB-231 cells), and total RNA was extracted. mRNA expression of a panel of luminal keratins and tight junction proteins was then assessed by real-time PCR. Results are shown as average mRNA expression relative to control treatment. N=3 tumors per condition.

C. Western blot to assess protein levels after MDA-MB-231 cells treatment in vitro as described in panel A. Beta-actin was used as a positive control. Representative images are shown from two separate experiments.

D. Immunohistochemistry of tumor sections for keratin 8 (KRT8) and claudin 7 (CLDN7) in the tumors treated as described in panel B. Representative images are shown from three separate tumors per group.

E. In vitro invasion was measured in matrigel-coated transwells for control or stably overexpressing CLDN7, CLDN11 or OCLN MDA-MB-231 cell lines in the presence of TGFβ and/or control IgG or the inhibitory antibody to human CSF1R. Results are shown as relative number of invaded cells normalized to the control cell line. N=3 separate experiments with duplicate transwells. In vitro proliferation was measured by EdU incorporation for the control and the overexpression cells lines, again in presence or absence of TGFβ and/or control IgG or the inhibitory antibody to human CSF1R. Results are shown as the relative number of EdU-positive nuclei over total (by DAPI staining) normalized to the control cell line. N=2 separate experiments with triplicate plates.

Error bars: Mean ± SEM. *: $p<0.05$, **: $p<0.01$, ***: $p<0.001$ (by Student's t-test). KRT8: keratin 8, KRT19: keratin 19, CLDN3: claudin 3, CLDN4: Claudin 4, CLDN7, claudin 7; CLDN11: claudin 11, OCLN: occludin.

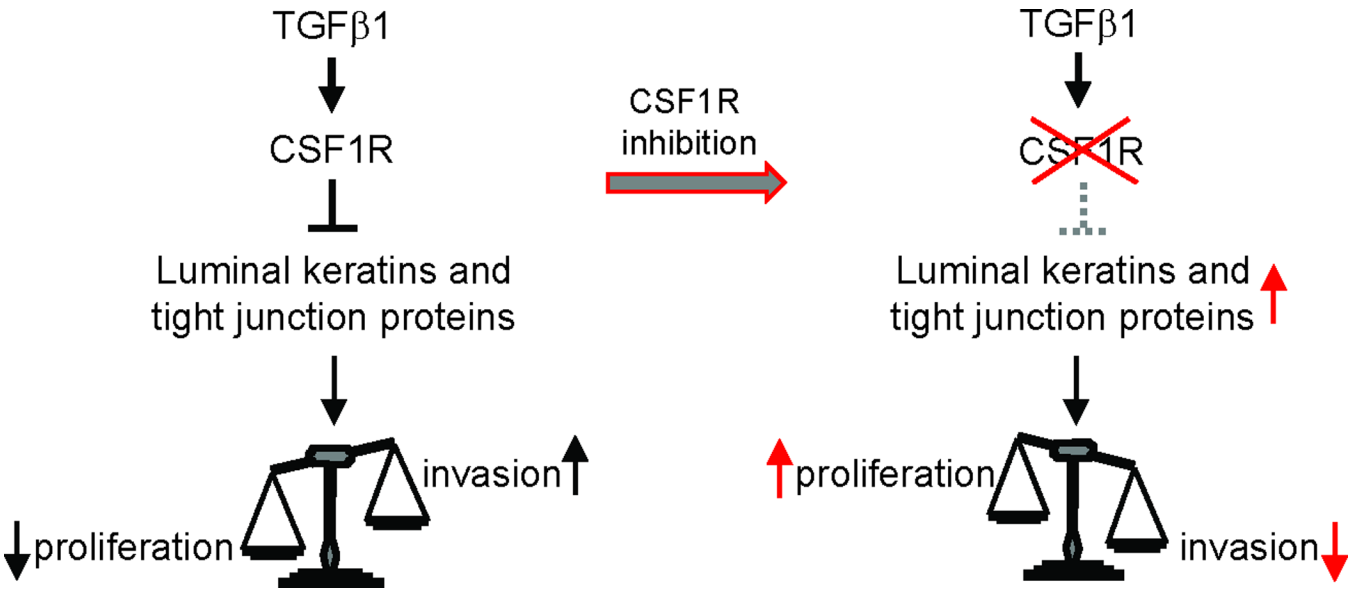

Figure 8. Model for the role of autocrine CSF1R signaling in claudin-low breast tumor cells

In claudin-low breast tumor cells, TGFβ signaling leads to upregulation of CSF1R. Autocrine CSF1R is a main signal for maintaining the breast tumor cells in a "claudin-low" state, by repressing expression of claudins and luminal keratins. As an end phenotype, autocrine CSF1R signaling regulates the balance between the "go or grow" states of the claudin-low breast tumor cells. When CSF1R signaling is inhibited, mRNA expression of claudins and luminal keratins is increased and the cells change from a "low growth-increased invasion" phenotype to an "increased growth-low invasion" phenotype.